HHS Public Access

Author manuscript

Biochem Pharmacol. Author manuscript; available in PMC 2022 March 12.

Published in final edited form as:

Biochem Pharmacol. 2022 March ; 197: 114910. doi:10.1016/j.bcp.2022.114910.

Cannabidiol Promotes Adipogenesis of Human and Mouse Mesenchymal Stem Cells via PPARγ by Inducing Lipogenesis but Not Lipolysis

Richard C. Chang[1], **Chloe S. Thangavelu**[1], **Erika M. Joloya**[1], **Angela Kuo**[1], **Zhuorui Li**[1], **Bruce Blumberg**[1,2,3,4]

[1]Department of Developmental and Cell Biology, University of California, Irvine, CA, USA, 92697-2300

[2]Department of Pharmaceuctical Sciences, University of California, Irvine, CA, USA, 92697-2300

[3]Department of Biomedical Engineering, University of California, Irvine, CA, USA, 92697-2300

1. Introduction

Cannabidiol (CBD) is a component of cannabis that is devoid of the typical psychotropic effects of the plant caused by its better known relative, Δ9-tetrahydrocannabinol (THC) [1]. Whereas THC mediates its effects on the brain and peripheral tissue through activation of the classical G-protein-coupled cannabinoid receptors, cannabinoid CB1 and cannabinoid CB2 [2], CBD does not significantly activate either of these receptors [3]. CBD has also been shown to antagonize the psychoactive effects of THC by blocking its conversion to the more psychoactive 11-hydroxy-THC [4] and to have antipsychotic, anti-anxiety effects [5, 6]. In addition to its anxiolytic properties, cannabidiol has been shown to have analgesic [7], anti-inflammatory [8, 9], anti-oxidant [10], and anti-cancer capabilities [10, 11].

Due to the increased availability of CBD-containing products after the recent legalization of commercial hemp and the legalization and/or decriminalization of cannabis in many US states, a growing number of individuals are exposed to CBD. Exposure is through commercially available CBD-containing products and recreational marijuana use. 37 million Americans aged 12 years or older reported using cannabis in 2018 [12]. Consumption of a single 1g marijuana cigarette resulted in a blood serum CBD concentration of up to 56.1 ng/mL (0.178 μM) [13]. Individuals can be exposed to higher and more continuous doses through prescribed medical treatments. For instance, CBD is now used in pharmaceutical products, such as the first cannabinoid-based drug developed, Sativex, to treat neuropathic pain in individuals with multiple sclerosis[14], rheumatoid arthritis [15], and cancer unresponsive to opiates [7]. In addition, the widespread availability of CBD-containing products across all 50 states has increased the overall exposure to CBD.

[4]To whom correspondence should be addressed. Bruce Blumberg, 2011 BioSci 3, University of California Irvine, Irvine, CA 92697, Phone (949) 824-8573, blumberg@uci.edu.

The molecular targets of CBD have been studied in an attempt to determine the mechanisms underlying its medicinal benefits. It is thought that CBD may mediate its effects by interacting with a variety of non-endocannabinoid receptors [16], such as the GPR55 Receptor [17], serotonin 5HT1A receptors [18, 19], Adenosine A2A receptors [20], and the vanilloid receptors TRPV1, TRPV2, TRPA1 [21]. However a growing body of evidence indicates that many effects of CBD, notably its anti-inflammatory and anti-cancer actions, can be inhibited by PPARγ antagonists suggesting that these actions may be PPARγ-dependent [22–28].

Peroxisome proliferator activated receptor gamma (PPARγ) is a member of a family of nuclear receptors containing three distinct subtypes: PPARα, PPARδ and PPARγ [29]. PPARγ is primarily involved in the regulation of adipocyte differentiation and lipid storage [30]. PPARs bind to DNA sequences and regulate the expression of target genes after heterodimerizing with the retinoid X receptor (RXR) [31] PPARs are endogenously activated by unsaturated fatty acids such as linolenic acid, linoleic acid, petroselenic acid and arachidonic acid [32]. PPARγ is capable of binding and being activated by a wide variety of structurally diverse ligands including organotins such as the biocide tributyltin (TBT) [33], phthalates which are commonly found in plastics [34], and thioglitazones [35]. Thiazolidinediones are a class of pharmaceutical PPARγ-selective agonists that includes the drug rosiglitazone (ROSI), which was once used to treat insulin resistance and decrease blood glucose levels in type 2 diabetes [36]. Like cannabidiol, PPARγ ligands exhibit anti-inflammatory actions, including the upregulation of anti-inflammatory cytokines and the downregulation of pro-inflammatory cytokines and nitric oxide synthase (iNOS) expression [37]. Other cannabinoids such as THC [38], ajulemic acid, a structural analog of a THC metabolite [39], and the endocannabinoids anandamide and 2-arachidonoylglycerol (2-AG) bind to PPARγ [40] or have anti-inflammatory and other effects that can be inhibited with PPARγ antagonists [41, 42]. Taken together, these reports indicate that CBD, like other cannabinoid and pharmaceutical PPARγ activators, may exert some of its physiological effects via a PPARγ-dependent mechanism.

To assess whether CBD could regulate another important PPARγ-dependent process we tested whether CBD promoted adipocyte differentiation in human and mouse multipotent mesenchymal stromal stem cells (a.k.a., MSCs). We found that CBD induced adipogenesis in MSCs by binding to and activating PPARγ and that inhibition of PPARγ with an antagonist also inhibited the adipogenic effects of CBD. These data confirm that CBD is a PPARγ agonist and that PPARγ activation may underlie the adipogenic effects of cannabidiol. These results are consistent with the possibility that consumption or use of CBD could lead to increased accumulation of white adipose tissue.

2. Materials and Methods

2.1. Chemicals

TBT, LG100268, dexamethasone, insulin, isobutylmethylxanthine, Nile Red, Hoechst 33342 were purchased from Sigma-Aldrich (St. Louis, MO). ROSI was purchased from Cayman Chemical (Ann Arbor, MI). T0070907 was purchased from Enzo Life Sciences (Farmingdale, NY). Formaldehyde was purchased from Thermo Fisher Scientific (Waltham,

MA). 99% pure CBD crystals were purchased from CBDistillery and diluted to 200 mM in DMSO for storage.

2.2. Cell Culture

hTERT immortalized adipose derived mesenchymal stem cells (ATCC SCRC-4000) were purchased from ATCC (Manassas, VA) and stored at passage 4 in liquid N_2. Bone marrow–derived multipotent MSCs from the long bones of C57BL/6J mice (MSCs) were purchased at passage 6 (OriCell; Cyagen Biosciences, Santa Clara, CA) and stored at passage 8 or 9 in liquid N_2. Bone marrow-derived human MSCs were purchased from Promocell (Lot 429Z001) and stored in liquid N_2. Cells were maintained, as previously described [43], in Dulbecco's modified Eagle medium containing 10% calf bovine serum, 10 mM HEPES, 1 mM sodium pyruvate, 100 IU/mL penicillin, and 100 μg/mL streptomycin. MSCs were plated at 15,000 cells/cm^2 in 12-well cell culture plates. For standard adipogenesis assays, cells were allowed to attach and acclimate for 24 hours prior to 48 hours of chemical treatment (day −2 through day 0). Specific ligands [200 nM ROSI, 50 nM TBT, 200 nM LG268 or CBD (100 nM - 10 μM)] were dissolved in DMSO and administered every 3 days throughout the duration of the assay. Antagonist assays were performed in parallel under the same conditions, but the antagonist T0070907 (100 nM-1 μM) or DMSO vehicle control was added every 12 hours. The amount of dimethyl sulfoxide (DMSO) vehicle was kept at <0.1% in all assays. No changes in cell viability were observed at the chemical doses used in this study.

2.3. Adipogenesis and Staining

Once they reached 100% confluency, cells were induced to differentiate with an adipose induction cocktail (500 μM isobutylmethylxanthine, 1 μM dexamethasone, and 5 μg/mL insulin) in minimal essential medium α containing 15% fetal bovine serum, 10 mM HEPES, 2 mM l-glutamine, 100 IU/mL penicillin, and 100 μg/mL streptomycin as we described [44]. Cells were replenished with fresh media, differentiation factors, and chemical ligands every 3 days, then fixed in buffered 3.7% formaldehyde. Cells were differentiated over the course of 14 days for murine MSC cell lines and 21 days for human MSCs.

Nile Red (1 μg/mL) was used to stain neutral lipids and Hoechst 33342 (1 μg/mL) to stain DNA. Cells were fixed with 3.7% formadehyle, washed once with PBS for 1 minute, and maintained at 4°C in PBS overnight to remove residual phenol red. For each biological replicate, Nile Red relative fluorescence units (RFU) was measured relative to Hoechst RFU using a SpectraMax Gemini XS spectrofluorometer (Molecular Devices, Sunnyvale, CA) using SoftMax Pro (Molecular Devices) [45].

2.4. RNA Isolation and Real-Time RT-qPCR Analysis of Gene Expression

Differentiated adipocytes were lysed with TriPure (Roche, Basel, Switzerland). Total RNA extracted with chloroform (Fisher Chemical, PA), precipitated with isopropanol (Fisher Chemical, PA). Complementary DNA was synthesized from 1 μg total RNA using reverse transcriptase (Roche), according to the manufacturer's instructions. Gene expression was assessed with real-time quantitative polymerase chain reaction (qPCR) using SYBR™ Green PCR Master Mix (Thermo Fisher Scientific, MA) on a Roche LightCycler 480 II

(Roche). Cycle threshold values were quantified as the second derivative maximum using LightCycler software (Roche). The $2^{-\Delta\Delta Ct}$ method [46] was used to analyze RT-qPCR data and determine relative quantification. Standard propagation of error was used throughout for each treatment group [47]. The data were normalized to a housekeeping gene, the ribosomal protein 36B4, and compared to 0.1% DMSO vehicle for standard assays or a 0.1% DMSO vehicle plus T0070907 for antagonist assays. Error bars represent the SEM from three to four biological replicates, calculated using standard propagation of error [47]. Each assay was conducted at least twice.

2.5. Transient Transfection Assays

Nuclear receptor activation by CBD was tested using the luciferase reporter tk-(ApoA1)x4-luc, pCMX-β-galactosidase [48] and fusion constructs to nuclear receptor ligand-binding domains for human PPARγ and RXRα [49]. Transient transfections were performed as described [50] in COS7 cells (ATCC® CRL-1,651™). Briefly, COS7 cells were seeded in Dulbecco's Modified Eagle Medium (DMEM; HyClone) containing 10% CBS at a density of 15,000 cells per well in 96-well tissue culture plates. After becoming 90% confluent approximately 24 hours after seeding, cells were transfected in Opti-MEM® using Lipofectamine® 2000 reagent (Invitrogen™; Life Technologies), according to the manufacturer's recommended protocol. One microgram of effector plasmid, five micrograms of reporter, and five micrograms of pCMX-β-galactosidase [48] transfection control plasmids per 96-well plate and incubated overnight. Cells were then treated with ligands or vehicle control in DMEM containing 10% resin charcoal stripped FBS for an additional 24 hours[51]. In transient transfection assays, the control compounds ROSI (PPARγ agonist), LG268 (RXR agonist), and TBT (PPARγ and RXR agonist) were tested from 10^{-10} M to 10^{-5} M, whereas CBD was tested up to 10^{-4} M to account for its weaker capacity as an agonist. Cells were lysed in 165 μl of lysis buffer [25 mM Tris-phosphate (pH 7.8), 15% glycerol, 2% 3-((3-cholamidopropyl) dimethylammonio)-1-propanesulfonate (CHAPS), 1% lecithin, 1% bovine serum albumin (BSA), 4 mM ethylene glycol-bis(β-aminoethyl ether)-N, N, N′, N′-tetraacetic acid (EGTA), 6 mM Magnesium Chloride ($MgCl_2$), 1 mM dithiothreitol (DTT), 1 mM and 4-(2- aminoethyl)benzenesulfonyl fluoride hydrochloride (AEBSF)]. 24 h after adding the ligands to the media, media was removed and lysis buffer added, then cells were placed on a shaker at room temperature for 30 min. For luciferase assays, 100 μl of luciferase solution [4.28 mM magnesium carbonate hydroxide pentahydrate ((MgCO3)4Mg(OH)25H2O), 10.68 mM magnesium sulfate (MgSO4), 80 mM Tricine (pH 7.8), 0.4 mM ethylendinitrilo tetraacetic acid (EDTA) (pH 8.0), 5 mM DTT, 0.15 mg/mL Coenzyme A, 0.5 mM adenosine triphosphate (ATP), and 0.5 mM D-Luciferin] and 50 μl of the lysate from each well was transferred to a well in a nontreated, white, flat-bottom, polystyrene, 96-well plate (Costar). The plate was shaken for 30 s at RT and placed in Dynatech ML3000 luminometer. Luminescence for the reporter was measured with luminometer ML3000 (version 3.07) software. For β-galactosidase assay, 100 μl of β-galactosidase solution [60 mM sodium phosphate dibasic (Na_2HPO4), 40 mM sodium phosphate monobasic (NaH_2PO_4), 10 mM potassium chloride (KCl), and 1 mM magnesium chloride ($MgCl_2$), 0.3% β-Mercaptoethanol, and 0.5–3 mg/mL o-nitrophenyl β-D-galactopyranoside (ONPG)] and 50 μl of the cell lysate was transferred to a clear, 96-well plate (Thermo Fisher Scientific, MA). The plates were placed on a shaker for 30 seconds

and allowed to incubate at room temperature for 15 minutes. A Versamax microplate reader (Molecular Devices) was used to measure absorbance at a wavelength of 405 nm using SOFTmaxPRO 4.0 software.

2.6. Statistical Analysis

GraphPad Prism 7.0 (GraphPad Software, Inc.) was used to perform statistical analysis for all datasets. A one-way analysis of variance (ANOVA) followed by Dunnett's post-hoc test was performed to compare the different concentrations of CBD to the vehicle and an unpaired t-test was performed to compare the positive controls ROSI, TBT, LG268 to the vehicle in adipogenesis assays. In antagonist assays, treatment groups without T0070907 were compared to a corresponding treatment group treated with T0070907 using a student's t-test. $P \leq 0.05$ was considered statistically significant.

3. Results

3.1. CBD activates PPARγ but not RXRα to induce adipogenesis in human and mouse model *in vitro*

Accumulated studies showed the effects of CBD may be mediated through a variety of non-endocannabinoid receptors; however, nuclear receptors such as PPARγ and RXRα were not well-studied. We tested the effects of CBD on PPARγ and its heterodimeric partner, RXR in transient transfection assays using luciferase reporter genes. Statistically significant activation of human and mouse PPARγ started from 100 nM CBD, which was similar in potency to the positive control, 100 nM ROSI, albeit with much lower efficacy (Figure 1A,1C). However, CBD showed no activity toward RXRα (Figure 1B, 1D). In addition, compare to ROSI, we noticed CBD has the same maximal effect at 100 nM but with a lower efficacy which suggests that CBD is a potential and partial agonist of PPARγ. With the presence of 100 nM ROSI or CBD, CBD and ROSI still showed a dose dependent response in both human and mouse PPAR (Figure 1E, 1F). PPARγ is known to be a key regulator of adipogenesis. Therefore, we tested whether CBD promoted adipogenesis by activating PPARγ by testing the ability of CBD to induce adipogenesis in MSCs and if any activity observed could be inhibited by co-treatment with the selective PPARγ antagonist, T0070907. In human cells, CBD showed a dose-dependent effect on adipogenesis which was suppressed by 100 nM T0070907 (Figure 1G). In mouse cells, both 5 and 10 μM CBD increased adipogenesis; 100 nM T0070907 significantly suppressed this induction (Figure 1H).

3.2. CBD enhanced adipogenesis by increasing expression of lipogenic genes

During adipogenesis, increased expression of adipogenic markers such as PPARγ2, fatty acid binding protein-4 (FABP4), and fat-specific protein-27 (FSP27) promote lipid accumulation. We performed adipogenesis assays on human MSCs using CBD (2.5, 5, or 10 μM), compared with 100 nM ROSI, 50 nM TBT, or 100nM LG268 as positive controls. In hMSCs, Nile Red staining revealed a dose-dependent increase in lipid accumulation by CBD (Figure 2A). Expression levels of mRNAS encoding three adipogenic genes, PPARG2, FABP4, and FSP27 were increased by both CBD and the PPARγ agonist, ROSI, whereas TBT and LG268 failed to increase expression of PPARγ2 mRNA (Figure 2B–D).

In mMSCs, 2.5 μM CBD did not increase lipid accumulation after a 14-day adipogenesis assay but 5 and 10 μM CBD did (Figure 2E). All of three doses of CBD increased PPARγ2 mRNA levels but FABP4 and FSP27 genes responded to CBD only at 10 μM (Figure 2F–H). TBT and LG268 did not induce PPARγ2 expression in hMSCs or mMSCs (Fig 2B & 2F).

3.3. CBD showed no effects on lipolysis or expression of lipolysis genes during adipogenesis

During adipogenesis, cells utilize both lipogenic and lipolytic pathways to acquire fatty acids and reach a net balance to accumulate fat content. Although ROSI induced the expression of the lipolysis genes, adipose triglyceride lipase (PNPLA2) and hormone-sensitive lipase (LIPE), CBD treatment did not alter expression of PNPLA2 or LIPE mRNAs in human MSCs (Figure 3C–D). We measured the free fatty acid content in the culture medium by the end of 14-day adipogenesis assay and found that ROSI and TBT groups showed increased free fatty acid level in the medium whereas the 10 μM CBD treated group accumulated less compared to controls (Figure 3A). To examine lipolytic function, isoproterenol was added to induce lipolysis in adipocytes differentiated with DMSO, 100 nM ROSI, 50 nM TBT, or 100nM LG268. Isoproterenol increased free fatty acid levels in the culture medium whereas CBD showed no differences responding to isoproterenol (Figure 3B). Similarly, CBD did not affect lipolysis gene expression or free fatty acid accumulation in the culture medium of mMSCs (Figure 3E–H).

3.4. The PPARγ antagonist T0070907 suppressed CBD-induced lipogenic gene expression in both human and mouse MSCs

After excluding the association between CBD-induced PPARγ activation and lipolysis, we next tested whether the expression of lipogenesis genes, FABP4, FSP27 and PPARG2 in response to CBD treatment was dependent on PPARγ by treating with the PPARγ antagonist, T0070907. ROSI and TBT induced the expression of lipogenesis genes in hMSCs and served as positive controls. 5 and 10μM CBD induced expression of the lipogenesis genes which were significantly suppressed by co-treatment with the PPARγ antagonist (Figure 4A–C). Lipogenesis genes were also induced by ROSI and CBD in mMSCs. In our study, we observed that T0070907 was able to suppress the effects of ROSI and CBD close to the baseline suggesting PPARγ plays a dominant role in CBD induced lipogenesis gene expression. Collectively, these observations indicate that CBD can promote adipogenesis by regulating lipogenesis but not lipolysis in both human and mouse MSCs.

4. Discussion

The purpose of this study was to determine the effects of cannabidiol on adipogenesis in mouse and human MSCs and whether this can be attributed to PPARγ activation. We found that CBD activates PPARγ in transient transfection assays and promoted the differentiation of human MSC's into adipocytes. The action of CBD could be inhibited by co-treatment with the PPARγ antagonist T0070907. These results are consistent with previous findings which showed that CBD promoted differentiation of mouse 3T3-L1 preadipocytes into adipocytes [52]. CBD had a stronger adipogenic effect in the human adipose-derived MSCs than in mouse MSCs. This suggests that although mouse body weight did not change to

a significant extent following 30 mg/kg CBD exposure [53], this might not be the case for humans exposed to CBD in commercial products with concentrations above 5 μM. In addition, the mouse study did not examine body composition (% fat vs % lean); and we previously demonstrated that the obesogen tributyltin could elicit increased white adipose tissue weight without increasing total body weight [44]. Other PPARγ activators, such as rosiglitazone and pioglitazone, were associated with human weight gain [36, 54] and the gene expression analyses showed that CBD-induced adipogenesis genes including PPARG2, FABP4, and FSP27. Taken together, these studies indicated that CBD acts as a weak PPARγ agonist in MSCs and up-regulates target genes, resulting in an increase in adipogenesis.

Two major processes in adipogenesis are lipogenesis and lipolysis which contribute to a net balance of triglyceride accumulation in fat cells. Lipogenesis is the processes of fatty acid synthesis and subsequent triglyceride synthesis, which take place in both liver and adipose tissues [55]. FABP4 encodes the fatty acid binding protein found in adipocytes. Fatty acid binding proteins binds long-chain fatty acids and other hydrophobic ligands to perform fatty acid uptake, transport, and metabolism [56]. Fat-specific protein 27 (FSP27) was reported to promote lipid droplet expansion by lipid trafficking at lipid droplet contact sites [57]. These two lipogenesis markers were positively regulated by PPARγ to enhance adipogenesis [58]. ROSI induced FABP4 and FSP27 expression which was abolished by PPARγ agonist as many reported. Our data showed that 10 μM CBD induced FABP4 and FSP27 expression (~3 fold and ~6 fold, respectively) in human MSCs. We also observed similar induction of FABP4 and FSP27 expression (~10 fold and ~7 fold, respectively) in mouse MSCs. Those effects of CBD were all suppressed by the PPARγ antagonist, T0070907, suggesting that PPARγ responds to CBD and further promotes lipogenesis. Surprisingly, we found that CBD showed no effects on lipolysis genes, PNPLA2 and LIPE, which were induced by ROSI in our study and in other reports [59]. We confirmed this observation by validating the lipolysis capacity of adipocytes matured by treating MSCs with CBD, ROSI, TBT, and LG. However, the strong lipolysis inducer, isoproterenol, induced lipolysis well in all groups, including CBD groups, which showed no changes in lipolysis gene expression. We therefore inferred that CBD regulated lipogenesis but not lipolysis during adipogenesis in both human and mouse MSCs.

Several studies have suggested CBD can act as an agonist for PPARγ[60–62]. For example, Fellous T's group use mice bone marrow derived mesenchymal stem cells to examine the effects of CBD including adipocytes regulatory genes and insulin induced AKT phosphorylation[62]. Our findings revealed a similar effect of CBDs and further tested the effects of both murine and human models. In addition, our data excluded the effects of CBD in lipolysis and re-enforced the role of lipogenesis in CBD-induced adipogenesis.

Taken together, our findings indicate that CBD has the ability to promote adipogenesis in mouse and human MSCs and that this may be the result of it inducing lipogenesis that is not balanced by lipolysis. Our findings will help in understanding possible unexpected effects resulting from the widespread use of CBD in both recreational cannabis and in personal care products.

References

1. O'Sullivan SE, et al. , Time-dependent vascular actions of cannabidiol in the rat aorta. Eur J Pharmacol, 2009. 612(1–3): p. 61–8. [PubMed: 19285060]
2. Pertwee RG, Pharmacology of cannabinoid CB1 and CB2 receptors. Pharmacol Ther, 1997. 74(2): p. 129–80. [PubMed: 9336020]
3. Howlett AC, et al. , International Union of Pharmacology. XXVII. Classification of Cannabinoid Receptors. Pharmacological Reviews, 2002. 54(2): p. 161–202. [PubMed: 12037135]
4. Russo E and Guy GW, A tale of two cannabinoids: the therapeutic rationale for combining tetrahydrocannabinol and cannabidiol. Med Hypotheses, 2006. 66(2): p. 234–46. [PubMed: 16209908]
5. Moreira FA, Aguiar DC, and Guimaraes FS, Anxiolytic-like effect of cannabidiol in the rat Vogel conflict test. Prog Neuropsychopharmacol Biol Psychiatry, 2006. 30(8): p. 1466–71. [PubMed: 16876926]
6. Zuardi AW, et al. , Cannabidiol, a Cannabis sativa constituent, as an antipsychotic drug. Brazilian Journal of Medical and Biological Research, 2006. 39: p. 421–429. [PubMed: 16612464]
7. Johnson JR, et al. , Multicenter, double-blind, randomized, placebo-controlled, parallel-group study of the efficacy, safety, and tolerability of THC:CBD extract and THC extract in patients with intractable cancer-related pain. J Pain Symptom Manage, 2010. 39(2): p. 167–79. [PubMed: 19896326]
8. Costa B, et al. , The non-psychoactive cannabis constituent cannabidiol is an orally effective therapeutic agent in rat chronic inflammatory and neuropathic pain. Eur J Pharmacol, 2007. 556(1–3): p. 75–83. [PubMed: 17157290]
9. Esposito G, et al. , Cannabidiol in vivo blunts beta-amyloid induced neuroinflammation by suppressing IL-1beta and iNOS expression. Br J Pharmacol, 2007. 151(8): p. 1272–9. [PubMed: 17592514]
10. Garcia-Arencibia M, et al. , Evaluation of the neuroprotective effect of cannabinoids in a rat model of Parkinson's disease: importance of antioxidant and cannabinoid receptor-independent properties. Brain Res, 2007. 1134(1): p. 162–70. [PubMed: 17196181]
11. Ligresti A, et al. , Antitumor activity of plant cannabinoids with emphasis on the effect of cannabidiol on human breast carcinoma. J Pharmacol Exp Ther, 2006. 318(3): p. 1375–87. [PubMed: 16728591]
12. Steigerwald S, et al. , Smoking, Vaping, and Use of Edibles and Other Forms of Marijuana Among U.S. Adults. Annals of Internal Medicine, 2018. 169(12): p. 890–892. [PubMed: 30167665]
13. Pacifici R, et al. , THC and CBD concentrations in blood, oral fluid and urine following a single and repeated administration of "light cannabis". Clin Chem Lab Med, 2019.
14. Rog DJ, et al. , Randomized, controlled trial of cannabis-based medicine in central pain in multiple sclerosis. Neurology, 2005. 65(6): p. 812–9. [PubMed: 16186518]
15. Blake DR, et al. , Preliminary assessment of the efficacy, tolerability and safety of a cannabis-based medicine (Sativex) in the treatment of pain caused by rheumatoid arthritis. Rheumatology (Oxford), 2006. 45(1): p. 50–2. [PubMed: 16282192]
16. Ibeas Bih C, et al. , Molecular Targets of Cannabidiol in Neurological Disorders. Neurotherapeutics, 2015. 12(4): p. 699–730. [PubMed: 26264914]
17. Ryberg E, et al. , The orphan receptor GPR55 is a novel cannabinoid receptor. Br J Pharmacol, 2007. 152(7): p. 1092–101. [PubMed: 17876302]
18. Russo EB, et al. , Agonistic properties of cannabidiol at 5-HT1a receptors. Neurochem Res, 2005. 30(8): p. 1037–43. [PubMed: 16258853]
19. Pazos MR, et al. , Mechanisms of cannabidiol neuroprotection in hypoxic-ischemic newborn pigs: role of 5HT(1A) and CB2 receptors. Neuropharmacology, 2013. 71: p. 282–91. [PubMed: 23587650]
20. Carrier EJ, Auchampach JA, and Hillard CJ, Inhibition of an equilibrative nucleoside transporter by cannabidiol: a mechanism of cannabinoid immunosuppression. Proc Natl Acad Sci U S A, 2006. 103(20): p. 7895–900. [PubMed: 16672367]

21. Costa B, et al. , Vanilloid TRPV1 receptor mediates the antihyperalgesic effect of the nonpsychoactive cannabinoid, cannabidiol, in a rat model of acute inflammation. Br J Pharmacol, 2004. 143(2): p. 247–50. [PubMed: 15313881]
22. O'Sullivan SE, Kendall DA, and Randall MD, Time-dependent vascular effects of Endocannabinoids mediated by peroxisome proliferator-activated receptor gamma (PPARgamma). PPAR Res, 2009. 2009: p. 425289. [PubMed: 19421417]
23. Esposito G, et al. , Cannabidiol reduces Abeta-induced neuroinflammation and promotes hippocampal neurogenesis through PPARgamma involvement. PLoS One, 2011. 6(12): p. e28668. [PubMed: 22163051]
24. De Filippis D, et al. , Cannabidiol reduces intestinal inflammation through the control of neuroimmune axis. PLoS One, 2011. 6(12): p. e28159. [PubMed: 22163000]
25. Ramer R, et al. , COX-2 and PPAR-gamma confer cannabidiol-induced apoptosis of human lung cancer cells. Mol Cancer Ther, 2013. 12(1): p. 69–82. [PubMed: 23220503]
26. Scuderi C, Steardo L, and Esposito G, Cannabidiol promotes amyloid precursor protein ubiquitination and reduction of beta amyloid expression in SHSY5YAPP+ cells through PPARgamma involvement. Phytother Res, 2014. 28(7): p. 1007–13. [PubMed: 24288245]
27. Hegde VL, et al. , Critical Role of Mast Cells and Peroxisome Proliferator-Activated Receptor gamma in the Induction of Myeloid-Derived Suppressor Cells by Marijuana Cannabidiol In Vivo. J Immunol, 2015. 194(11): p. 5211–22. [PubMed: 25917103]
28. Hind WH, England TJ, and O'Sullivan SE, Cannabidiol protects an in vitro model of the blood-brain barrier from oxygen-glucose deprivation via PPARgamma and 5-HT1A receptors. Br J Pharmacol, 2016. 173(5): p. 815–25. [PubMed: 26497782]
29. Ferre P, The biology of peroxisome proliferator-activated receptors: relationship with lipid metabolism and insulin sensitivity. Diabetes, 2004. 53 Suppl 1: p. S43–50. [PubMed: 14749265]
30. Tontonoz P and Spiegelman BM, Fat and beyond: the diverse biology of PPARgamma. Annu Rev Biochem, 2008. 77: p. 289–312. [PubMed: 18518822]
31. Kliewer SA, et al. , Convergence of 9-cis retinoic acid and peroxisome proliferator signalling pathways through heterodimer formation of their receptors. Nature, 1992. 358(6389): p. 771–4. [PubMed: 1324435]
32. Kliewer SA, et al. , Fatty acids and eicosanoids regulate gene expression through direct interactions with peroxisome proliferator-activated receptors alpha and gamma. Proc Natl Acad Sci U S A, 1997. 94(9): p. 4318–23. [PubMed: 9113987]
33. le Maire A, et al. , Activation of RXR-PPAR heterodimers by organotin environmental endocrine disruptors. EMBO Rep, 2009. 10(4): p. 367–73. [PubMed: 19270714]
34. Hurst CH and Waxman DJ, Activation of PPARalpha and PPARgamma by environmental phthalate monoesters. Toxicol Sci, 2003. 74(2): p. 297–308. [PubMed: 12805656]
35. Lehmann JM, et al. , An antidiabetic thiazolidinedione is a high affinity ligand for peroxisome proliferator-activated receptor gamma (PPAR gamma). J Biol Chem, 1995. 270(22): p. 12953–6. [PubMed: 7768881]
36. Rangwala SM and Lazar MA, Peroxisome proliferator-activated receptor gamma in diabetes and metabolism. Trends Pharmacol Sci, 2004. 25(6): p. 331–6. [PubMed: 15165749]
37. Szeles L, Torocsik D, and Nagy L, PPARgamma in immunity and inflammation: cell types and diseases. Biochim Biophys Acta, 2007. 1771(8): p. 1014–30. [PubMed: 17418635]
38. O'Sullivan SE, et al. , Novel time-dependent vascular actions of Delta9-tetrahydrocannabinol mediated by peroxisome proliferator-activated receptor gamma. Biochem Biophys Res Commun, 2005. 337(3): p. 824–31. [PubMed: 16213464]
39. Liu J, et al. , Activation and binding of peroxisome proliferator-activated receptor gamma by synthetic cannabinoid ajulemic acid. Mol Pharmacol, 2003. 63(5): p. 983–92. [PubMed: 12695526]
40. Gasperi V, et al. , Endocannabinoids in adipocytes during differentiation and their role in glucose uptake. Cell Mol Life Sci, 2007. 64(2): p. 219–29. [PubMed: 17187172]
41. Rockwell CE and Kaminski NE, A cyclooxygenase metabolite of anandamide causes inhibition of interleukin-2 secretion in murine splenocytes. J Pharmacol Exp Ther, 2004. 311(2): p. 683–90. [PubMed: 15284281]

42. Rockwell CE, et al. , Interleukin-2 suppression by 2-arachidonyl glycerol is mediated through peroxisome proliferator-activated receptor gamma independently of cannabinoid receptors 1 and 2. Mol Pharmacol, 2006. 70(1): p. 101–11. [PubMed: 16611855]
43. Shoucri BM, et al. , Retinoid X Receptor Activation Alters the Chromatin Landscape To Commit Mesenchymal Stem Cells to the Adipose Lineage. Endocrinology, 2017. 158(10): p. 3109–3125. [PubMed: 28977589]
44. Chamorro-Garcia R, et al. , Ancestral perinatal obesogen exposure results in a transgenerational thrifty phenotype in mice. Nat Commun, 2017. 8(1): p. 2012. [PubMed: 29222412]
45. Shoucri BM, et al. , Retinoid X Receptor Activation During Adipogenesis of Female Mesenchymal Stem Cells Programs a Dysfunctional Adipocyte. Endocrinology, 2018. 159(8): p. 2863–2883. [PubMed: 29860300]
46. Livak KJ and Schmittgen TD, Analysis of relative gene expression data using real-time quantitative PCR and the 2(-Delta Delta C(T)) Method. Methods, 2001. 25(4): p. 402–8. [PubMed: 11846609]
47. Bevington PR, Robinson DK, and Bunce G, Data Reduction and Error Analysis for the Physical Sciences, 2nd ed. American Journal of Physics, 1993. 61(8): p. 766–767.
48. Forman BM, et al. , Unique response pathways are established by allosteric interactions among nuclear hormone receptors. Cell, 1995. 81(4): p. 541–50. [PubMed: 7758108]
49. Chamorro-Garcia R, et al. , Effects of Perinatal Exposure to Dibutyltin Chloride on Fat and Glucose Metabolism in Mice, and Molecular Mechanisms, in Vitro. Environ Health Perspect, 2018. 126(5): p. 057006. [PubMed: 29787037]
50. Janesick AS, et al. , On the Utility of ToxCast and ToxPi as Methods for Identifying New Obesogens. Environ Health Perspect, 2016. 124(8): p. 1214–26. [PubMed: 26757984]
51. Chamorro-Garcia R, et al. , Bisphenol A diglycidyl ether induces adipogenic differentiation of multipotent stromal stem cells through a peroxisome proliferator-activated receptor gamma-independent mechanism. Environ Health Perspect, 2012. 120(7): p. 984–9. [PubMed: 22763116]
52. Vallee A, et al. , Effects of cannabidiol interactions with Wnt/beta-catenin pathway and PPARgamma on oxidative stress and neuroinflammation in Alzheimer's disease. Acta Biochim Biophys Sin (Shanghai), 2017. 49(10): p. 853–866. [PubMed: 28981597]
53. Carvalho RK, et al. , Chronic cannabidiol exposure promotes functional impairment in sexual behavior and fertility of male mice. Reprod Toxicol, 2018. 81: p. 34–40. [PubMed: 29936126]
54. Strowig SM and Raskin P, The effect of rosiglitazone on overweight subjects with type 1 diabetes. Diabetes Care, 2005. 28(7): p. 1562–7. [PubMed: 15983301]
55. Schwarz JM, et al. , Short-term alterations in carbohydrate energy intake in humans. Striking effects on hepatic glucose production, de novo lipogenesis, lipolysis, and whole-body fuel selection. J Clin Invest, 1995. 96(6): p. 2735–43. [PubMed: 8675642]
56. Furuhashi M, et al. , Fatty Acid-Binding Protein 4 (FABP4): Pathophysiological Insights and Potent Clinical Biomarker of Metabolic and Cardiovascular Diseases. Clin Med Insights Cardiol, 2014. 8(Suppl 3): p. 23–33.
57. Keller P, et al. , Fat-specific protein 27 regulates storage of triacylglycerol. J Biol Chem, 2008. 283(21): p. 14355–65. [PubMed: 18334488]
58. Garin-Shkolnik T, et al. , FABP4 attenuates PPARgamma and adipogenesis and is inversely correlated with PPARgamma in adipose tissues. Diabetes, 2014. 63(3): p. 900–11. [PubMed: 24319114]
59. Jin D, et al. , Lipocalin 2 is a selective modulator of peroxisome proliferator-activated receptor-gamma activation and function in lipid homeostasis and energy expenditure. FASEB J, 2011. 25(2): p. 754–64. [PubMed: 20974668]
60. Jung T, et al. , Functional interactions between cannabinoids, omega-3 fatty acids, and peroxisome proliferator-activated receptors: Implications for mental health pharmacotherapies. Eur J Neurosci, 2020.
61. Sonego AB, et al. , Cannabidiol prevents haloperidol-induced vacuos chewing movements and inflammatory changes in mice via PPARgamma receptors. Brain Behav Immun, 2018. 74: p. 241–251. [PubMed: 30217539]

62. Fellous T, et al. , Phytocannabinoids promote viability and functional adipogenesis of bone marrow-derived mesenchymal stem cells through different molecular targets. Biochem Pharmacol, 2020. 175: p. 113859. [PubMed: 32061773]

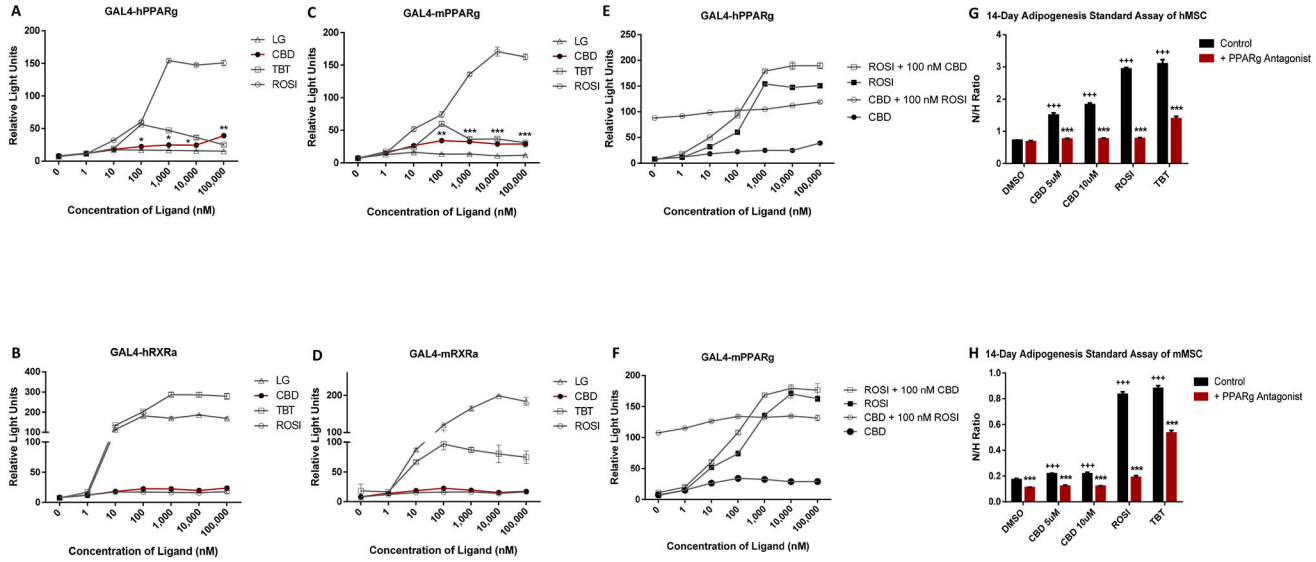

Figure 1. CBD bound to PPARγ and induce adipogenesis in human and mice MSC.

(A) The ability of CBD to activate PPARγ and RXRα was assessed in COS7 cells transiently transfected with luciferase reporter plasmid and either human PPARγ and (B) RXRα. (C) The ability of CBD to activate PPARγ and RXRα was assessed in COS7 cells transiently transfected with luciferase reporter plasmid and either mouse PPARγ and (D) RXRα. (E) The ability of CBD or ROSI to activate PPARγ with the presence of ROSI or CBD, respectively, was assessed in COS7 cells transiently transfected with luciferase reporter plasmid and either human PPARγ and (F) mouse PPARγ. The PPARγ activators ROSI and TBT were used as positive controls for activation of PPARγ, while the RXR activators LG268 and TBT were used as positive controls for activation of RXRα. Luciferase values were normalized to β-galactosidase transfection values to account for transfection efficiency. Triplicates for each chemical and concentration were averaged and plotted with ± SEM bars. (G) A standard adipogenesis assay was performed in human and (H) mouse MSCs in the presence of adipogenesis cocktail (MDI). Cells were treated with CBD (5μM or 10μM), a 100 nM ROSI, or 50 nM TBT, positive control with or without PPARγ antagonist, 100 nM T0070907. All treatment groups were compared to 0.1% DMSO (vehicle). Lipid accumulation is shown as the ratio between fluorescence units (RFU) of Nile Red and Hoechst, which were used to quantify lipid content and the number of cells per well, respectively. Each bar represents the average of 3 replicates ± SEM *P < 0.05, **P < 0.01 and ***P < 0.001 compared to control; ƒ P < 0.05, ƒƒ P < 0.01 and ƒƒƒ P < 0.001 compared to control). One-way analysis of variance (ANOVA) statistical test and a Dunnett's post-hoc test were performed to compare the different concentrations of CBD to DMSO.

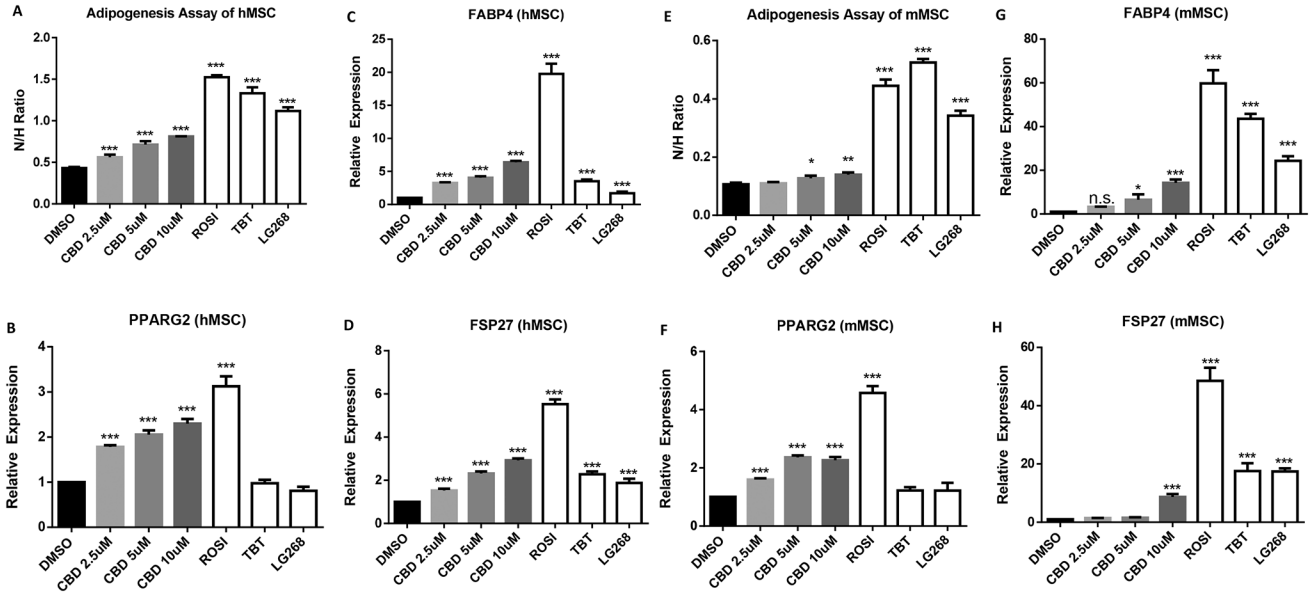

Figure 2. CBD enhanced adipogenesis and induced lipogenesis gene in human and mouse MSC.

(A) A standard adipogenesis assay was performed in human MSC in the presence of adipogenesis cocktail (MDI). Cells were treated with CBD (2.5μM, 5, or 10μM), a 100 nM ROSI, 50 nM TBT, or 100nM LG268 positive control. All treatment groups were compared to 0.1% DMSO (vehicle). Lipid accumulation is shown as the ratio between fluorescence units (RFU) of Nile Red and Hoechst, which were used to quantify lipid content and the number of cells per well, respectively. Each bar represents the average of 3 replicates ± SEM. (B) qRT-PCR validation of lipogenesis genes, PPARG2, (C) FABP4, and (D) FSP27, of human MSC differentiated adipocytes. (E) A standard adipogenesis assay was performed in the mouse MSC. (F) qRT-PCR validation of lipogenesis genes, PPARG2, (G) FABP4, and (H) FSP27, of mouse MSC differentiated adipocytes. For qRT-PCR analyses, measured Ct values were normalized to 36B4 and graphed relative to the control treatment. Error bars represent SEM *P < 0.05, **P < 0.01 and ***P < 0.001). Data analyzed using either an unpaired t-test or a one-way ANOVA followed by Dunnett's post hoc analysis.

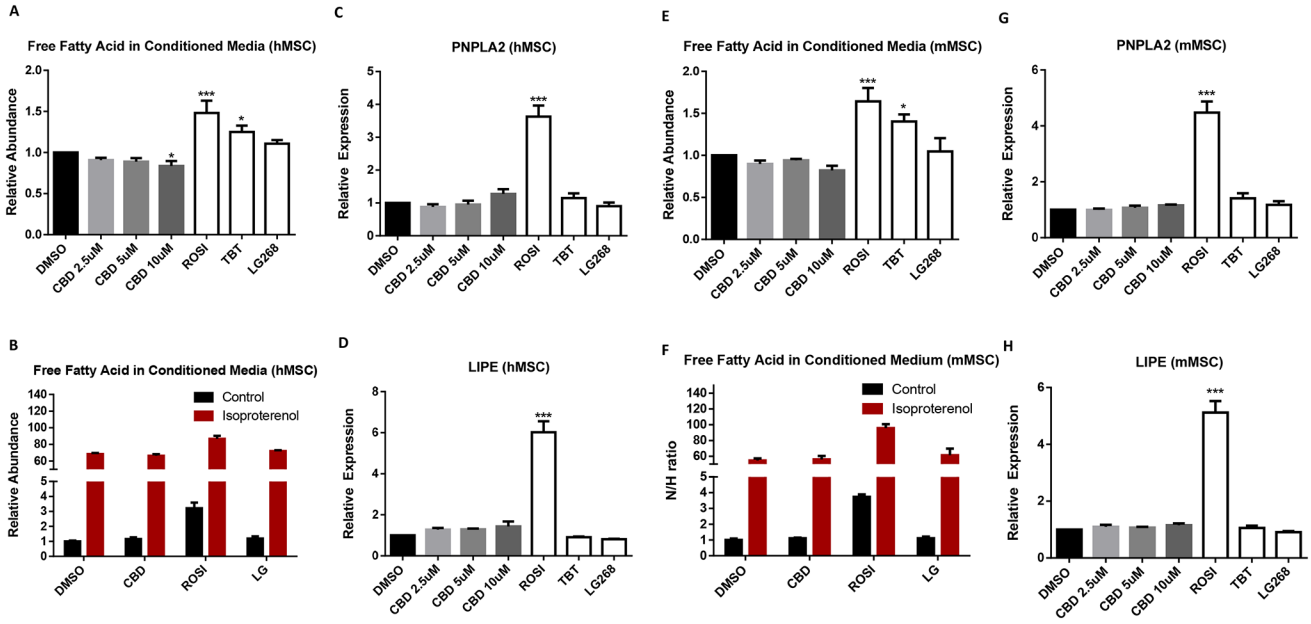

Figure 3. CBD did not affect lipolysis in human or mouse MSC.

(A) The cultured medium of human MSC at the end of adipogenesis or (B) 24 hours post-isoproterenol treatment after 14-day adipogenesis were collected to measure free fatty acids levels. (C) qRT-PCR validation of lipolysis genes, PNPLA2 and (D) LIPE, of human MSC differentiated adipocytes. (E) The cultured medium of mouse MSC at the end of adipogenesis or (F) 24 hours post-isoproterenol treatment after 14-day adipogenesis were collected to measure free fatty acids levels. (G) qRT-PCR validation of lipolysis genes, PNPLA2 and (H) LIPE, of mouse MSC differentiated adipocytes. For qRT-PCR analyses, measured Ct values were normalized to 36B4 and graphed relative to the control treatment. Error bars represent SEM *P < 0.05, **P < 0.01 and ***P < 0.001). Data analyzed using either an unpaired t-test or a one-way ANOVA followed by Dunnett's post hoc analysis.

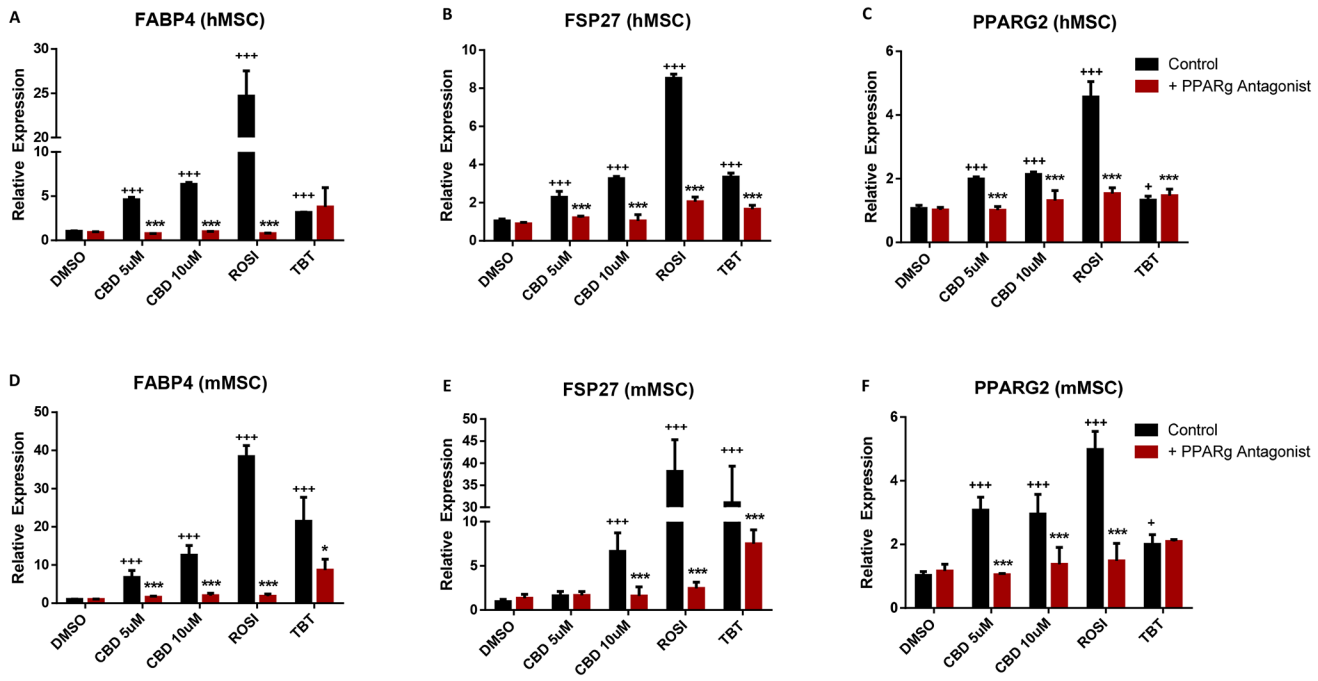

Figure 4. CBD-induced adipogenesis was inhibited by PPARγ antagonist T0070907 in human and mouse MSCs.

(A) qRT-PCR validation of lipogenesis genes, FABP4, (B) FSP27, and (C)PPARG2 of human MSC differentiated adipocytes. (D) qRT-PCR validation of lipogenesis genes, FABP4, (E) FSP27, and (F)PPARG2 of mouse MSC differentiated adipocytes. For qRT-PCR analyses, measured Ct values were normalized to 36B4 and graphed relative to the control treatment. Error bars represent 3 replicates ± SEM *P < 0.05 (**P < 0.01 and ***P < 0.001 compared to control; ǂ P < 0.05, ǂǂ P < 0.01 and ǂǂǂ P < 0.001 compared to control). Data analyzed using either an unpaired t-test or a one-way ANOVA followed by Dunnett's post hoc analysis.